Radio frequency transmitter based on a laser frequency comb

Marco Piccardo[a,1], Michele Tamagnone[a,1], Benedikt Schwarz[a,b], Paul Chevalier[a], Noah A. Rubin[a], Yongrui Wang[c], Christine A. Wang[d], Michael K. Connors[d], Daniel McNulty[d], Alexey Belyanin[c], and Federico Capasso[a,2]

[a]Harvard John A. Paulson School of Engineering and Applied Sciences, Harvard University, Cambridge, MA 02138; [b]Institute of Solid State Electronics, Technische Universität Wien, 1040 Wien, Austria; [c]Department of Physics and Astronomy, Texas A&M University, College Station, TX 77843; and [d]Lincoln Laboratory, Massachusetts Institute of Technology, Lexington, MA 02420

Contributed by Federico Capasso, March 19, 2019 (sent for review March 1, 2019; reviewed by Theodor W. Haensch and Jerome Faist)

Since the days of Hertz, radio transmitters have evolved from rudimentary circuits emitting around 50 MHz to modern ubiquitous Wi-Fi devices operating at gigahertz radio bands. As wireless data traffic continues to increase, there is a need for new communication technologies capable of high-frequency operation for high-speed data transfer. Here, we give a proof of concept of a compact radio frequency transmitter based on a semiconductor laser frequency comb. In this laser, the beating among the coherent modes oscillating inside the cavity generates a radio frequency current, which couples to the electrodes of the device. We show that redesigning the top contact of the laser allows one to exploit the internal oscillatory current to drive a dipole antenna, which radiates into free space. In addition, direct modulation of the laser current permits encoding a signal in the radiated radio frequency carrier. Working in the opposite direction, the antenna can receive an external radio frequency signal, couple it to the active region, and injection lock the laser. These results pave the way for applications and functionality in optical frequency combs, such as wireless radio communication and wireless synchronization to a reference source.

laser frequency comb | microwave generation | wireless emission

Optical fields can be used to synthesize low-phase noise microwaves by means of different techniques, such as optical frequency division (1, 2), optoelectronic oscillations (3), and laser heterodyne (4). The latter can be realized in a medium with a nonlinear optical response, such as a photomixer (5), capable of converting the frequency difference between the optical modes into a microwave tone (6–8). An attractive aspect of quantum cascade lasers (QCLs) operating as optical frequency combs (9–16) is that they can act both as sources of light with a spectrum that consists of equidistant modes and as photomixers—provided that their gain dynamics are sufficiently fast—producing microwaves of high spectral purity directly inside the laser cavity. The physical process underlying the microwave generation originates from the beating among neighboring optical modes of the standing wave cavity, which creates spatiotemporal variations of optical intensity inside the resonator. By means of stimulated emission and absorption, the modulated intensity creates a time-dependent population inversion grating that oscillates in time at the beat note frequency and presents a sinusoidal spatial pattern along the cavity. Opposite ends of this dynamic electronic grating oscillate nearly in antiphase at the beat frequency (Fig. 1*A*). Such a mechanism was used to demonstrate a quadrature modulation scheme exploiting the alternating currents oscillating inside the laser and a system of near-field microwave probes (17).

In light of this phenomenon, the laser can be viewed from a different perspective, namely as an ensemble of two radio frequency generators with a π-phase shift. Usually, the top electrode of these lasers consists of an electrically continuous metal contact connecting the two generators and thus, preventing the device from radiating. In this work, we demonstrate that adapting the geometry of the top contact layer of a QCL allows one to feed a dipole antenna on the chip, enabling emission of radio waves into free space. The beat note frequency itself can be tuned by modulating the laser current; thus, the laser acquires the functionality of turning into a radio transmitter capable of wireless communication at a carrier frequency of 5.5 GHz given by the comb repetition rate. Thanks to their fast gain recovery dynamics (18), QCLs have the potential of generating subterahertz carriers when operating in the harmonic comb regime with a wide intermodal spacing (19). The extension of the design presented here to realize a class of terahertz wireless communication devices (20–22) will be discussed.

Far-Field Emission of a Microwave Tone

The laser radio transmitter (LRT) is illustrated in Fig. 1*B*. It consists of a continuous wave, ridge waveguide, uncoated Fabry–Perot QCL with an 8-mm-long cavity operating as a fundamental frequency comb (12) in the mid-IR spectral range with a narrow (kilohertz) linewidth beat note at $f_B = 5.5$ GHz (Fig. 1*B*). A 400 -μm-wide gap is etched in the top contact layers of the device, creating two contact sections with an open circuit resistance of 250 Ω. The two top laser contacts are connected through wirebonds to a low-impedance half-wave dipole antenna designed to radiate at f_B consisting of two gold stripes fixed on a polyactide dielectric substrate. The laser current is injected from the dc power source through the antenna into the QCL (*Materials and Methods*).

Significance

Semiconductor lasers are compact sources of coherent light. When operating in an optical frequency comb regime, they can generate a spectrum consisting of discrete frequency lines that are equally spaced. Most frequency comb applications, such as spectroscopy and metrology, directly use the optical output of these lasers. In microwave photonics applications, the frequency comb output is sent to a fast photodetector and used to produce microwaves. Here, we propose to integrate laser, detector, and antenna in the same device. We show that, in addition to generating microwaves, a properly designed laser can emit microwaves wirelessly and modulate them with a signal containing information. This work opens the door to a type of hybrid electronic–photonic devices.

Author contributions: M.P., M.T., B.S., P.C., N.A.R., A.B., and F.C. designed research; M.P., M.T., B.S., P.C., N.A.R., Y.W., C.A.W., M.K.C., and D.M. performed research; M.P., M.T., and Y.W. analyzed data; and M.P., M.T., and F.C. wrote the paper.

Reviewers: J.F., ETH Zurich; and T.W.H., Max Planck Institute of Quantum Optics.

The authors declare no conflict of interest.

[1]M.P. and M.T. contributed equally to this work.

[2]To whom correspondence should be addressed. Email: capasso@seas.harvard.edu.

This article contains supporting information online at www.pnas.org/lookup/suppl/doi:10.1073/pnas.1903534116/-/DCSupplemental.

Published online April 24, 2019.

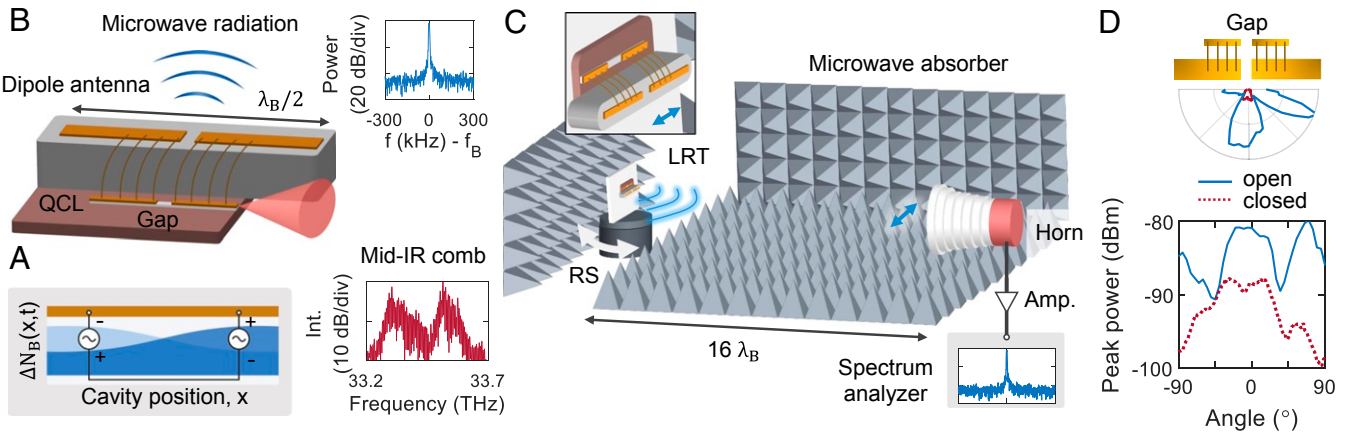

Fig. 1. (*A*) Schematic of the time-dependent population inversion grating oscillating inside the cavity of a QCL frequency comb at the fundamental beat note frequency. In light of this phenomenon, the laser can be regarded as two radio frequency generators oscillating in antiphase. (*B*) Introducing a gap in the design of the top electrode of the device allows one to use the radio frequency alternating currents generated inside the laser to feed a dipole antenna enabling wireless microwave emission in addition to the usual mid-IR radiation. *Insets* show the microwave beat note emitted from the device (*Upper Inset*; $f_B = 5.5$ GHz) and the mid-IR frequency comb spectrum (*Lower Inset*). (*C*) Setup for the characterization of the far-field pattern. The LRT is mounted on a rotation stage (RS), and the 5.5-GHz radiation emitted at different angles in the horizontal plane is measured at a distance of 0.9 m by a horn antenna connected to a spectrum analyzer. λ_B denotes the free space wavelength of the radiated beat note. Microwave absorbers are used to eliminate unwanted reflections from the surrounding environment. *Inset* shows a magnification of the LRT with the polarization of the emitted microwave field (double-headed arrow), which is the same one as the receiving horn antenna. (*D*) The radiation patterns are measured in the case where the gaps of the QCL and dipole antenna are open and closed by wirebonds. The direction normal to the surface of the LRT defines the 0° angle. Polar plots are shown with power plotted on a linear scale. The amplifier gain has been subtracted.

To characterize the emission pattern of the system, we carry out far-field measurements of the QCL microwave radiation. A schematic of the experimental setup is shown in Fig. 1*C*. The LRT is mounted on a rotation stage, and the microwave radiation emitted at angles between −90° and 90° on the horizontal plane is detected by a directive horn antenna (gain of 18.5 dBi) at a distance of 0.9 m (16 λ_B) from the source, amplified, and then, measured with a spectrum analyzer (*SI Appendix*). Fig. 1*D* shows the measured radiation pattern of the device (Fig. 1*D*, continuous line). The central peak observed around 0° originates from the dipole antenna and QCL, while the side lobes are due to emission from the wirebonds (*SI Appendix*). The maximum radiated power is approximately −80 dBm. When the gap of the QCL and antenna is closed using wirebonds (Fig. 1*D*, dashed line), the maximum power drops to −88 dBm. Although this does not correspond to the case of an unstructured device with a continuous metal electrode— because of the inductive nature of the wirebonds, which prevents them from being a perfect short—this result shows the fundamental role that the gap geometry plays for the wireless emission.

From the measured microwave radiation, taking into account the directivity of the emitter and receiver antenna and using an equivalent circuit model of the LRT, we can estimate the microwave power available at the source. The QCL active region can be modeled as a radio frequency generator with low-output impedance. The bonding pads on the sides of the waveguide behave as capacitors in parallel to the generator. A full model of the impedance of the pads and of the other elements in the equivalent circuit is described in *SI Appendix*. The antenna is connected to the QCL via wirebonds, the inductive behavior of which at microwave frequencies is also taken into account in the model. Finally, the antenna constitutes the load connected at the other end of the circuit. The impedance mismatch loss (mostly caused by the presence of the capacitive pads) is estimated to be −22 dB, which means that the power actually radiated by the antenna is 22 dB lower than the available power at the QCL. Using this fact and knowing that the total received power is −80 dBm, it is possible to compute the wireless link power budget with the Friis formula (*SI Appendix*). The total radiated power is found to be −58 dBm, meaning that the available power at the QCL is estimated to be −36 dBm. Based on numerical simulations of the QCL radio frequency generation, the available power is expected to increase by several orders of magnitude when operating the laser in the harmonic comb regime due to the higher optical power per mode and lower number of beat harmonics that are generated in this state (*SI Appendix*). The source impedance mismatch due to the pad admittance can be corrected using a buried heterostructure geometry with an iron-doped indium phosphide insulating layer (23), promising to improve the extraction performances both at microwave and subterahertz frequencies, as the capacitive pad admittance would be substantially reduced.

Wireless Transmission of an Audio Signal

Next, we provide a proof of concept of wireless communication using the LRT. Note that here information is encoded in the laser beat note rather than in an optical carrier as it was done in previous works in optical wireless communication (24). The experimental setup is schematized in Fig. 2*A*. The laser current is modulated by an audio analog signal, which in turn, modulates the frequency of the laser beat note, allowing it to encode the baseband information onto the 5.5-GHz carrier wave. The radio signal is received by a horn antenna at a distance of 0.9 m, filtered by a receiving filter (1.9- to 5.5-GHz bandwidth), amplified, and then, down-converted to 1.5 GHz by mixing with a local oscillator (LO; 7.0 GHz) to fit into the bandwidth of a software-defined radio (SDR) used for demodulation. The physical process underlying the current-driven beat note modulation is the following: the current modulation ΔI induces a thermal variation of the QCL active region, thus changing the group refractive index n_g of the cavity. This, in turn, changes the intermodal spacing of the comb and the beat note frequency. In Fig. 2*B*, we present a waterfall plot of the signal demodulated by the SDR when the laser current is modulated at $f_{mod} = 0.1$ Hz with a relative current modulation amplitude of $\Delta I/I = 0.2\%$. The beat note exhibits a nearly constant power, and its instantaneous frequency is modulated with a period of 10 s defined by f_{mod}, spanning a range of frequency deviation of 120 kHz determined by ΔI. In essence, the QCL behaves as a current-controlled oscillator,

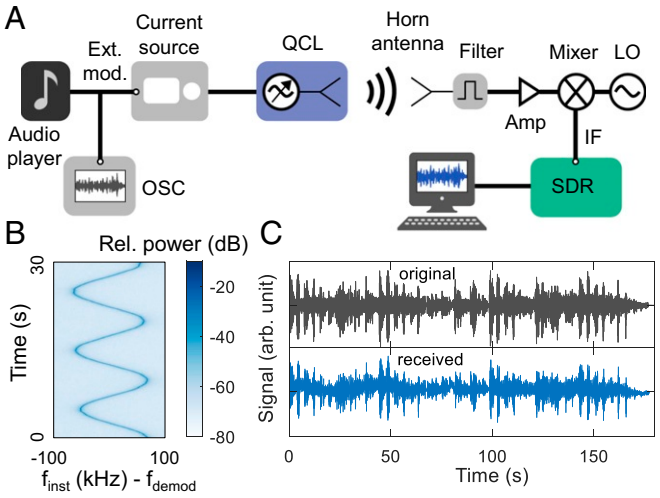

Fig. 2. (*A*) Setup for the wireless transmission and reception of an audio signal. The laser current is modulated by an analog signal inducing a frequency modulation of the laser beat note. The radio signal is received by a horn antenna, filtered, and down-converted to fit into the bandwidth of an SDR. IF, intermediate frequency; OSC, oscilloscope. (*B*) Waterfall plot showing the instantaneous frequency of the demodulated signal when the laser current is modulated at 0.1 Hz; it shows that the laser behaves as a current-controlled oscillator. (*C*) Original and received audio signal (Audio File S1 is the received audio file: "Volare" by Dean Martin).

which can generate a frequency-modulated (FM) signal. This scheme is used for radio transmission of an audio track, which can be correctly retrieved after demodulation (Fig. 2*C* and Audio File S1). Unwanted slow thermal fluctuations of the laser cavity, which persist despite the use of a temperature controller, induce a jittering of the beat note appearing as a slow modulation of the baseline of the received audio signal. The effect of these fluctuations is to add a noise contribution below 10 Hz (*SI Appendix*), which is outside of the audio frequency range (20–20,000 Hz). The high-frequency background noise that is audible in the track is due to the level of the noise floor. The signal-to-noise ratio could be improved by increasing the range of frequency deviation of the modulated beat note, although this was limited in this work by the bandwidth of the software demodulator. While this demonstration deals with a low-frequency audio modulation signal, QCL modulation of several tens of gigahertz has been demonstrated using microstrip and coplanar waveguide geometries (25–28). These studies investigated the high-frequency modulation of the optical field in single-mode QCLs and can aid in understanding the effect of multimode QCL modulation on the generated beat note, although additional research will be needed to assess the impact of high-power modulation on frequency combs. In particular, at gigahertz modulation frequencies, we expect that the laser beat note will be predominantly amplitude modulated by plasma effects, as the cutoff frequency of thermal effects responsible for frequency modulation is below 1 MHz (29, 30).

Wireless Locking to an External Radio Frequency Source

Due to the presence of the antenna, the laser is also sensitive to wireless radio frequency signals. Here, we show that the laser beat note can be wirelessly injection locked to an external microwave reference. A similar injection locking scheme was used in semiconductor mode-locked lasers equipped with patch antennas and operating in the telecommunication region for radio-over-fiber applications (31). A schematic of the setup is shown in Fig. 3*A*. An LO, tunable in power and frequency, is connected to a horn antenna directed at the QCL chip. A microwave probe is placed in proximity of the QCL antenna to monitor the changes in the laser beat note induced by the LO, the power of which is swept between −30 and 24 dBm for a set of different frequencies. Examples of the behavior exhibited by the QCL beat note on wireless microwave injection are shown in Fig. 3*B*. In the lower range of powers of the LO, the QCL behaves as free running; its beat note is unlocked and shows small-frequency oscillations around $f_0 = 5.501$ GHz due to thermal fluctuations. When the LO power overcomes a threshold dependent on the detuning from f_0, the QCL beat note locks to the external oscillator and stops jittering. This phenomenon is preceded by the appearance of a weaker sideband next to the QCL beat note as typically observed in wired injection locking experiments (26). The increase of the power threshold with the detuning from f_0 follows a quadratic dependence as expected from injection locking theory (32, 33). For the maximum explored power of the LO (24 dBm), the wireless locking range is about 40 kHz. We note that an enhancement of the microwave emission from the laser based on a buried heterostructure design as discussed above will also improve the coupling of external radio signals into the system, thus lowering the wireless locking threshold curve. The demonstration of wireless injection locking of the laser beat note shows the possibility

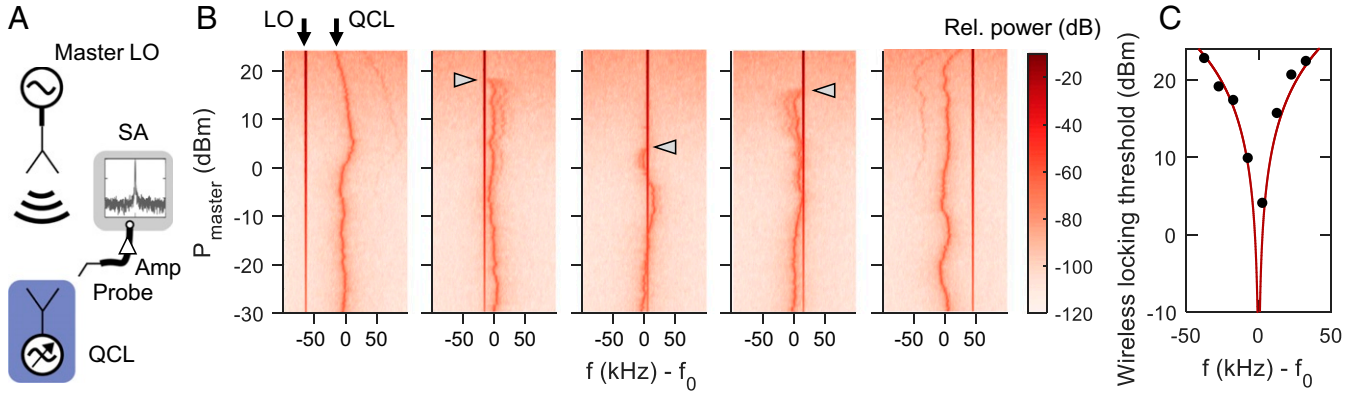

Fig. 3. (*A*) Schematic of the setup to injection lock the QCL beat note to an LO through free space. A probe placed near the antenna of the QCL monitors the changes in the laser beat note induced by the LO. The beat note is measured using a spectrum analyzer (SA). (*B*) Shift of the QCL beat note spectrum as the power of the LO is swept between −30 and 24 dBm. The LO power threshold at which locking occurs is marked by arrowheads. Frequencies are given with respect to the beat note frequency of the free-running QCL ($f_0 = 5.501$ GHz). Five exemplary cases are shown. (*C*) Measured LO power corresponding to the threshold for wireless locking of the QCL beat note to the LO for different LO frequencies (circles). Also shown is the fit of the theoretical quadratic dependence (continuous line).

of remote control of laser frequency combs and may open applications in the field, such as wireless synchronization of multiple comb generators to a single reference oscillator, without the need of integrating complex interconnected microwave architectures.

Discussion

This work is a proof of concept demonstration of a QCL frequency comb used as a wireless radio transmitter. Thanks to the recently discovered harmonic comb operation of QCLs (17, 19)—where the intermodal comb spacing is in the hundreds of gigahertz range due to longitudinal mode skipping—the frequency range of radio transmission of the system can be potentially extended to subterahertz carriers. Moreover, the frequency of such carriers holds promise of broad tunability, since the intermodal spacing of a harmonic frequency comb may be varied from a few 100 GHz up to over 1 THz in a single device, as it was recently experimentally demonstrated by optical injection of an external seed (34). In the harmonic regime, the internal dynamic grating will exhibit a number of spatial cycles corresponding to the number of skipped longitudinal modes in the frequency comb (17). Adapting the waveguide design demonstrated here to match the spatial periodicity of this higher-order grating will provide for extraction of a substantial fraction of the available radio frequency power generated in the harmonic state. For instance, traveling and standing wave antenna designs, which have already been proven successful in cryogenically cooled terahertz QCL systems (35, 36), or surface grating outcouplers used in difference frequency generation terahertz QCLs (37, 38) could be used to efficiently radiate the generated subterahertz signal. Other than increasing the carrier wave frequency, the harmonic state offers a spectrum of a few powerful optical modes. In principle, this spectral distribution of the optical power presents the net advantage of a much more efficient radio frequency generation for a given beat tone compared with QCLs operating in the fundamental comb regime, as it allows one to generate a radio frequency spectrum consisting of fewer but much stronger beat notes. Numerical simulations suggest that a QCL in the harmonic state can generate a beat note in the 100-GHz range with a 37-dB power enhancement with respect to that produced at 5.5 GHz by a QCL operating as a fundamental frequency comb in similar current and optical power conditions (*SI Appendix*). Considering that the available power at 5.5 GHz for the QCL studied in this work is −36 dBm, the estimated available power that would be obtained in the harmonic comb regime from this device is 1 dBm, which exceeds the −20-dBm level considered to be the lower limit for practical communication applications (22).

QCL radio frequency sources benefit from good impedance matching with extraction elements, such as antennas and waveguides, thanks to the low impedance of their active region. This is a clear advantage with respect to existing terahertz photomixers, which suffer from high impedance in the order of tens of kiloohm, thus losing several orders of magnitude in power efficiency. Thanks to the frequency comb nature of the light beating inside the cavity, this radio frequency source can generate tones of high spectral purity, leading to a very narrow (kilohertz or sub kilohertz) linewidth. Another attractive feature of the LRT is that the carrier frequency may be controlled by the laser current, allowing in principle to phase lock it to a reference microwave source using frequency division and thus, stabilize it with high accuracy. Ultimately, the system introduced here will benefit from unprecedented compactness compared with existing composite terahertz wireless communication systems (20), unifying in a single device the capability of room temperature generation, modulation, and emission of subterahertz waves, and it may find applications in fields ranging from telecommunications and spectroscopy to radioastronomy and quantum optics.

Materials and Methods

Laser and Antenna Design. The QCL has a layer structure consisting of GaInAs/AlInAs lattice matched to InP; it emits at 9.0 μm and is described in more detail in ref. 39. The 12-μm-wide QCL waveguide was fabricated by reactive ion etching followed by SiN passivation using plasma-enhanced chemical vapor deposition, sputtered Ti/Au contact deposition using a lift off, substrate thinning to 150 μm, bottom-side Ti/Au contact deposition, and cleaving to a 8-mm-long device. The device was soldered epitaxial side up with indium on a copper plate. The half-wave dipole antenna is designed for $f_B = 5.5$ GHz and consists of two gold metal stripes (each being 6.5-mm long and 2-mm wide) with a 1-mm gap lying on a 3D-printed polyactide substrate (3-mm thick, $\varepsilon_r = 2.7$). Each arm of the antenna is connected on one side to one of two QCL top pads using wirebonds and on the other side, to the negative connector of the current source via an inductor to minimize radio frequency (RF) leakage (*SI Appendix*, Fig. S2*C*). The QCL is operated in a fundamental (1 free spectral range intermodal spacing) frequency comb regime at an injected current of ∼1.82 A ($1.26I_{th}$) driven with a low-noise current driver (Wavelength Electronics QCL LAB 2000) and with its temperature stabilized at 16°C using a low-thermal drift temperature controller (Wavelength Electronics TC5). In this operating condition, the differential resistance of the QCL is estimated to be 1.3 Ω, and the emitted optical power per facet is 40 mW. Uncoupled modes of a free-running QCL typically generate a broad beat note with a megahertz linewidth and a high-phase noise pedestal. Here, the laser operates in a frequency comb regime with a kilohertz linewidth beat note, which is sufficiently narrow for the purpose of this demonstration. If required by the specific application, hertz-level beat note linewidths may be achieved in QCLs by additional improvements in the temperature and current stability of the laser and by control of its dispersion.

Microwave Far-Field Measurements. Far-field mapping has been performed by mounting a commercial directive horn antenna (RF Elements SH-CC 5-30) on the same optical table with the QCL transmitter at a distance of ∼0.9 m ($16\ \lambda_B$) from the QCL assembly. The antenna has a maximum gain of 18.5 dBi, negligible return loss at 5.5 GHz, and two separate ports for vertical and horizontal polarization, and it was aimed at the QCL transmitter. The latter is mounted on a motorized rotary stage, which allows for mapping of the far field in the horizontal plane. The optical table and other reflective surfaces nearby are covered with microwave absorbers (SFC-4 from Cuming Microwave) with less than 30 dB of reflectivity at 5.5 GHz. The output of the antenna (50 Ω) is connected to a low-noise preamplifier (19 dB of gain) and then, to a spectrum analyzer (Agilent E4448A). Stage and data acquisition are controlled by a computer.

Radio Transmission. The voltage signal generated by an audio player is used to modulate the laser current using the external analog modulation input of the current source (Wavelength Electronics QCL LAB 2000; analog current transfer function: 0.4 A/V). The volume of the audio player is chosen to set the maximum peak-to-peak output voltage to a value (0.2 V) such that the maximum frequency deviation of the modulated QCL beat note is within the demodulation bandwidth of the software-defined radio (RTL-SDR: R820T tuner frequency capability of 25–1,750 MHz; RTL2832U demodulator bandwidth of 200 kHz). A wideband FM demodulation scheme is used. With reference to Fig. 2*A*, the amplifier gain is 19 dB at 5.5 GHz, and the LO (Hittite HMC-T2240) power is 0 dBm.

Wireless Injection Locking. The master signal is generated by an LO (Hittite HMC-T2240) feeding a horn antenna (RF Elements SH-CC 5-30). To monitor the changes in the QCL beat note induced by the external oscillator signal, a coaxial RF probe (Quater A-20338; bandwidth dc 18 GHz; tip diameter ∼ 100 μm) is placed in the near field of the dipole antenna on the QCL chip (∼2 mm away from the edge of one of two arms). This arrangement is noninvasive (in the sense that the probe is not in electrical contact with the dipole antenna) and allows one to simultaneously monitor both the QCL RF beat note and the master radiated LO signal. The signal detected by the probe is amplified (19-dB gain) and measured with a spectrum analyzer (Agilent E4448A).

ACKNOWLEDGMENTS. We thank D. Kazakov for discussions that motivated this demonstration and a careful reading of the manuscript, and A. Amirzhan for useful discussions. We acknowledge support from NSF Award ECCS-1614631. The work conducted by Lincoln Laboratory was sponsored by Assistant Secretary of Defense for Research and Engineering Air Force Contracts FA8721-05-C-0002 and/or FA8702-15D-0001. This work was performed in part at the Center for Nanoscale Systems, a member of

the National Nanotechnology Coordinated Infrastructure Network, which is supported by NSF Award 1541959. M.T. acknowledges the support of Swiss National Science Foundation Grant 177836. B.S. was supported by Austrian Science Fund Project NanoPlas P28914-N27. N.A.R. is supported by NSF Graduate Research Fellowship Program Grant DGE1144152. Any opinions, findings, conclusions, or recommendations expressed in this material are those of the authors and do not necessarily reflect the views of the Assistant Secretary of Defense for Research and Engineering or the NSF.

1. Fortier TM, et al. (2011) Generation of ultrastable microwaves via optical frequency division. *Nat Photon* 5:425–429.
2. Li J, Yi X, Lee H, Diddams SA, Vahala KJ (2014) Electro-optical frequency division and stable microwave synthesis. *Science* 345:309–313.
3. Maleki L (2011) The optoelectronic oscillator. *Nat Photon* 5:728–730.
4. Li J, Lee H, Vahala KJ (2013) Microwave synthesizer using an on-chip Brillouin oscillator. *Nat Commun* 4:2097.
5. Tani M, Morikawa O, Matsuura S, Hangyo M (2005) Generation of terahertz radiation by photomixing with dual- and multiple-mode lasers. *Semicond Sci Tech* 20:S151–S163.
6. Kim J, Kärtner FX (2010) Microwave signal extraction from femtosecond mode-locked lasers with attosecond relative timing drift. *Opt Lett* 35:2022–2024.
7. Rubiola E, Santarelli G (2013) Frequency combs: The purest microwave oscillations. *Nat Photon* 7:269–271.
8. Quinlan F, et al. (2013) Exploiting shot noise correlations in the photodetection of ultrashort optical pulse trains. *Nat Photon* 7:290–293.
9. Schliesser A, Picqué N, Hänsch TW (2012) Mid-infrared frequency combs. *Nat Photon* 6:440–449.
10. Udem T, Holzwarth R, Hänsch TW (2002) Optical frequency metrology. *Nature* 416:233–237.
11. Hänsch TW (2006) Nobel lecture: Passion for precision. *Rev Mod Phys* 78:1297–1309.
12. Hugi A, Villares G, Blaser S, Liu HC, Faist J (2012) Mid-infrared frequency comb based on a quantum cascade laser. *Nature* 492:229–233.
13. Villares G, Hugi A, Blaser S, Faist J (2014) Dual-comb spectroscopy based on quantum-cascade-laser frequency combs. *Nat Commun* 5:5192.
14. Burghoff D, et al. (2014) Terahertz laser frequency combs. *Nat Photon* 8:462–467.
15. Lu QY, et al. (2015) High power frequency comb based on mid-infrared quantum cascade laser at $\lambda \sim 9\mu$m. *Appl Phys Lett* 106:51105.
16. Cappelli F, et al. (2016) Frequency stability characterization of a quantum cascade laser frequency comb. *Laser Photon Rev* 10:623–630.
17. Piccardo M, et al. (2018) Time-dependent population inversion gratings in laser frequency combs. *Optica* 5:475–478.
18. Choi H, et al. (2008) Gain recovery dynamics and photon-driven transport in quantum cascade lasers. *Phys Rev Lett* 100:167401.
19. Kazakov D, et al. (2017) Self-starting harmonic frequency comb generation in a quantum cascade laser. *Nat Photon* 11:789–792.
20. Nagatsuma T, Ducournau G, Renaud CC (2016) Advances in terahertz communications accelerated by photonics. *Nat Photon* 10:371–379.
21. Akyildiz IF, Jornet JM, Han C (2014) Terahertz band: Next frontier for wireless communications. *Phys Commun* 12:16–32.
22. Kleine-Ostmann T, Nagatsuma T (2011) A review on terahertz communications research. *J Infrared Millim Terahertz Waves* 32:143–171.
23. Nida S, Hinkov B, Gini E, Faist J (2017) Characterization of iron doped indium phosphide as a current blocking layer in buried heterostructure quantum cascade lasers. *J Appl Phys* 121:094502.
24. Capasso F, et al. (2002) Quantum cascade lasers: Ultrahigh-speed operation, optical wireless communication, narrow linewidth, and far-infrared emission. *IEEE J Quantum Electron* 38:511–532.
25. Maineult W, et al. (2010) Microwave modulation of terahertz quantum cascade lasers: A transmission-line approach. *Appl Phys Lett* 96:021108.
26. Gellie P, et al. (2010) Injection-locking of terahertz quantum cascade lasers up to 35GHz using RF amplitude modulation. *Opt Express* 18:20799–20816.
27. Calvar A, et al. (2013) High frequency modulation of mid-infrared quantum cascade lasers embedded into microstrip line. *Appl Phys Lett* 102:181114.
28. Hinkov B, Hugi A, Beck M, Faist J (2016) Rf-modulation of mid-infrared distributed feedback quantum cascade lasers. *Opt Express* 24:3294–3312.
29. Tombez L, et al. (2013) Wavelength tuning and thermal dynamics of continuous-wave mid-infrared distributed feedback quantum cascade lasers. *Appl Phys Lett* 103:031111.
30. Hangauer A, Spinner G, Nikodem M, Wysocki G (2014) High frequency modulation capabilities and quasi single-sideband emission from a quantum cascade laser. *Opt Express* 22:23439–23455.
31. Khawaja BA, Cryan MJ (2010) Wireless hybrid mode locked lasers for next generation radio-over-fiber systems. *J Lightwave Technol* 28:2268–2276.
32. Siegman AE (1986) *Lasers* (University Science Books, Sausalito, CA).
33. Adler R (1973) A study of locking phenomena in oscillators. *Proc IEEE* 61:1380–1385.
34. Piccardo M, et al. (2018) Widely tunable harmonic frequency comb in a quantum cascade laser. *Appl Phys Lett* 113:031104.
35. Tavallaee AA, Williams BS, Hon PWC, Itoh T, Chen Q-S (2011) Terahertz quantum-cascade laser with active leaky-wave antenna. *Appl Phys Lett* 99:141115.
36. Masini L, et al. (2017) Continuous-wave laser operation of a dipole antenna terahertz microresonator. *Light Sci Appl* 6:e17054.
37. Pflugl C, et al. (2008) Surface-emitting terahertz quantum cascade laser source based on intracavity difference-frequency generation. *Appl Phys Lett* 93:161110.
38. Kim JH, et al. (2018) Difference-frequency generation terahertz quantum cascade lasers with surface grating outcouplers. *Proceedings of the Conference on Lasers and Electro-Optics* (Optical Society of America, San Jose, CA), no. SF3G.7.
39. Wang CA, et al. (2017) MOVPE growth of LWIR AlInAs/GaInAs/InP quantum cascade lasers: Impact of growth and material quality on laser performance. *IEEE J Sel Top Quantum Electron* 23:1–13.

Correction

APPLIED PHYSICAL SCIENCES

Correction for "Radio frequency transmitter based on a laser frequency comb," by Marco Piccardo, Michele Tamagnone, Benedikt Schwarz, Paul Chevalier, Noah A. Rubin, Yongrui Wang, Christine A. Wang, Michael K. Connors, Daniel McNulty, Alexey Belyanin, and Federico Capasso, which was first published April 24, 2019; 10.1073/pnas.1903534116 (*Proc. Natl. Acad. Sci. U.S.A.* **116**, 9181–9185).

The authors note that the statement in the Acknowledgments "We acknowledge support from NSF Award ECCS-1614631" should instead appear as "We acknowledge support from the NSF under Awards CCSS-1807323 and ECCS-1614631."

Published online August 19, 2019.

www.pnas.org/cgi/doi/10.1073/pnas.1913679116